

# Visualization of downwellings in 3-D spherical mantle convection

Shuo Wang\*, Shuxia Zhang, David. A. Yuen

*University of Minnesota, Supercomputing Institute, 117 Pleasant Street SE, Minneapolis, MN 55455, United States*

Received 4 February 2007; accepted 20 March 2007

## Abstract

Although the Amira visualization package has been available since 1999, not much effort has been made to use this powerful package for addressing the challenging problem that geodynamicists have in visualizing 3-D features of cold downwellings in spherical mantle convection simulations with high spatial resolution. In this paper, we present three approaches that exploit the functionalities of Amira to meet the needs of visualizing the complexity of these dynamic processes. The first task is to use the multiple isosurfaces combined with different colors and transparencies for showing the large-scale features from a global perspective. The second task is to localize the small-scale features of interest by cutting off the rest or splitting off a small part of image from the entire picture so that the details can be viewed locally. The third one is the use of multiple windows simultaneously for showing different portions of the same set data in different displaying formats from various angles of view. We will also present new geophysical findings based on these visualization approaches.

© 2007 Elsevier B.V. All rights reserved.

*Keywords:* Scientific visualization; Downwellings; Amira

## 1. Introduction

Numerical simulations of 3-D spherical mantle convection (Glatzmaier, 1988; Bercovici et al., 1989) have played an important role for understanding the dynamical process of plate tectonics (Tackley et al., 2001) and the evolution of the Earth's mantle. Several spherical models of mantle convection have been available for over 20 years (e.g., Machetel et al., 1986; Baumgardner, 1985; Zhang and Yuen, 1995; Zhong et al., 2000). Much attention has been devoted to portraying the dynamics of upwellings and visualizing their structure and dynamical behavior. The cold downwelling processes play the same important roles as the upwellings in the dynamical processes of mantle convection, but not much work has

been devoted to the downwellings except in the works by H. Davies where he focused on the influences of the downwelling on interacting with the bottom thermal boundary layer and inducing secondary upwellings (Davies, 2005). The major obstacle is the spherical geometry constraint, which prevents an observer from viewing the downwellings from outside of the spherical shell. There is also the problem associated with the smaller volume of the lower mantle, where the downwellings are bunched up. Another method for viewing downwellings in 3-D spherical convection, albeit very expensive, is using immersive technology, such as the CAVE (Cruz-Neira et al., 1993), whereby one can peer at the descending slabs coming down from above.

The importance of visualization in comprehending the large datasets in the geosciences has already been stressed in the recent report on computational geo-

\* Corresponding author. Tel.: +1 651 324 4674.

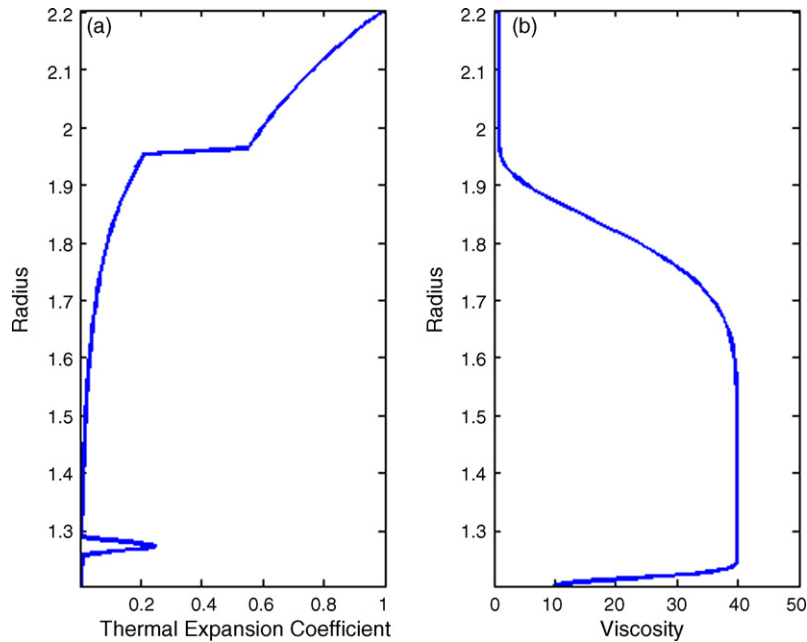


Fig. 1. (a) Dimensionless thermal expansion coefficient and (b) depth-dependent viscosity coefficient.

sciences by Cohen (2005). The objective of this research work was to develop a few graphic templates, which will help the geodynamical community better visualize and understand the dynamical process of downwellings. Certainly, these graphic approaches or the same ideas embedded in these approaches can also be applied to effectively and efficiently visualize complicated fluid dynamical processes in engineering and other geophysical fluid dynamical applications.

## 2. Methodology

### 2.1. Numerical model

For generating the data, we used the hybrid spectral-finite-difference code of 3-D spherical mantle convection developed by Zhang and Christensen (1993). This code solves time-dependent extended Boussinesq equations of mass, momentum and energy conservations for the fluids with infinite Prandtl number and three-dimensional variable viscosity. The datasets used for this manuscript are from the model with an averaged Rayleigh number of  $2 \times 10^6$ , a dimensionless thermal expansion coefficient (Fig. 1a) and a depth-dependent viscosity (Fig. 1b) subject to the isothermal free-slip boundary conditions. The model resolution consists of spherical harmonic degree and order of 320 and 200 higher-order finite difference points (Fornberg, 1996) in the radial direction.

### 2.2. Visualization approaches

We employed Amira 4.1 (<http://www.amiravis.com/>) to visualize the 3-D mantle convection results. Erlebacher et al. (2001) have described the use of Amira in the geosciences by means of numerous examples. Hanyk et al. (in press) have employed the Amira package in the post-glacial rebound problem and have presented a detailed description on making movies over structured and unstructured grids. Amira is a powerful commercial tool developed by Mercury Computer Systems available for Linux, Windows, and Macintosh. Amira provided many pre-written modules for different visualization functionalities in a simple user environment, where we uploaded the data, and applied pre-written modules to extract relevant information. The modules we have employed are Heightfield, Isosurface, ObliqueSlice, and TimeSeriesControl. More details on these modules are presented in the description of each of the visualization procedures below.

In the following graphic displays, the large-scale downwelling features are characterized by the temperature distribution in 3-D spherical coordinates. The data with value varying from 0 to 254 (corresponding to 0–3000 °C) are saved in the curvilinear format predefined in Amira. Each dataset contains the temperature distribution at a given step of the time sequences. Over 1000 of these data sets were generated from the entire time series of one single simulation. The size of each

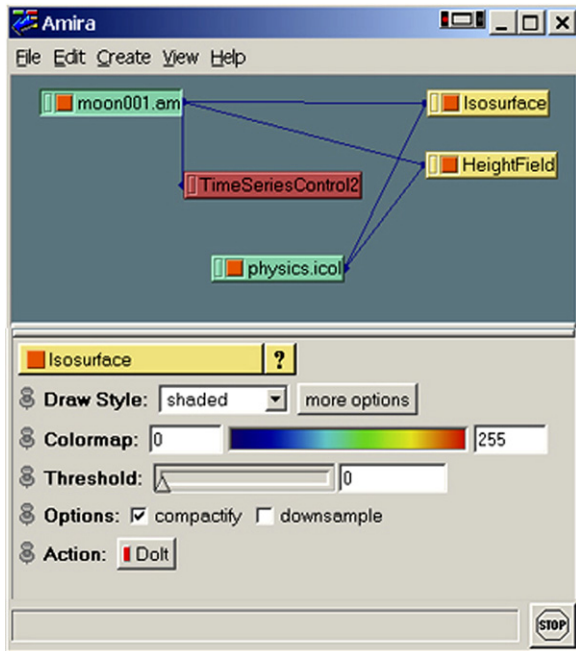


Fig. 2. A diagram showing Amira modules used for generating multiple iso-surfaces.

data set varies from 22 MB (downsampled by 2 on each side) to 178 MB (without downsampling).

### 2.2.1. Use of multiple isosurfaces

One of the virtues of Amira is the availability of the diagrammatic setup, displaying the various connecting modules. Fig. 2 is an example of such a diagram showing the selected modules and their connections for displaying the large-scale features. Moon001.am is the input dataset, which is connected to a time series control module. This module allows one to select one of the time series datasets for generating one snapshot. This module also allows Amira to cycle through each dataset automatically and re-update the image in the viewer.

After a dataset is uploaded, one can apply other display modules, such as HeightFields, ObliqueSlices, and Isosurfaces, to the dataset and adjust these modules to focus on specific thresholds of interest. For instance, to view the structure associated with the temperatures with a value of 55, one can generate an isosurface of temperature with a value of 55. Through the Isosurfaces model, one can select the colormap ('physics.icol' in Fig. 2) for this isosurface, and then change the alpha curve within the colormap to change the transparency of the isosurface. We can use the Isosurfaces module multiple times to create multiple isosurfaces, each of which is assigned with a specific value of temperature and a color. The colors can be the same or different. But the transparency of

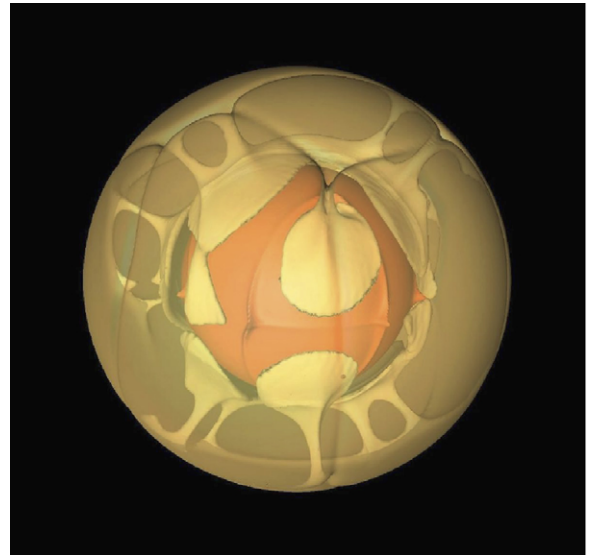


Fig. 3. A single isosurface showing the downwellings developed at the early time period when the convection started in an isoviscous model with a Rayleigh number of  $3 \times 10^5$ .

the isosurfaces must decrease exponentially with temperature or toward an inner part of one or a few particular downwellings so that the inner structures can be well revealed. Repeating adjustments are needed to achieve the best visual effects. This can be seen in Fig. 4. After the multi-isosurfaces is set for one dataset, one can use the same setting through the time control module to efficiently produce movie for all the datasets that the time control module can access.

Fig. 3 shows a snapshot of the downwellings developed at the early time period in an isoviscous convection model with a Rayleigh number ( $Ra$ ) of  $3 \times 10^5$  subject to the initial condition that small lateral perturbations are placed in the mantle with a conductive or a radially dependent temperature profile. We believe this is the first time from the visualization perspective that we have been able to show the clear presence of both linear and circular downwelling structures in the 3-D spherical model.

The image in Fig. 3 demonstrates that the multi-isosurfaces approach can be used to examine how the cold flows are formed and how they move from the surface into the deep mantle subject to various dynamical conditions. Certainly this graphic approach can also be used for displaying the structures of the upwellings. Fig. 4 shows two images from different angles of view of the convection model with  $Ra = 2 \times 10^6$  and thermal expansion coefficient (Fig. 1a) and radially dependent viscosity (Fig. 1b). In addition, the multi-isosurfaces approach provides a cost-efficient way to mimic the volume-rendering of 3-D features. Volume-rendering

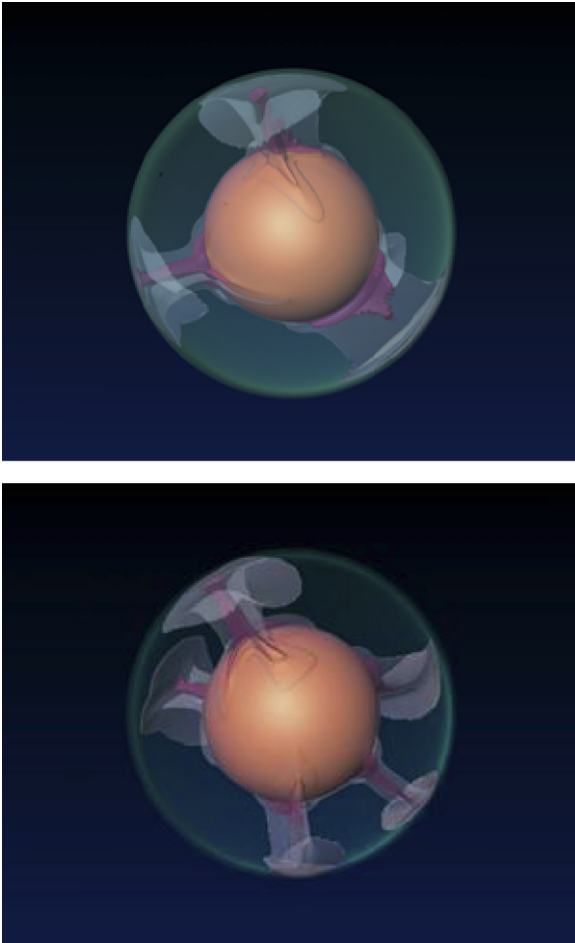


Fig. 4. Visualization of upwellings from two different perspectives. The four isosurfaces (green, white, purple, and orange) are respectively associated with 0, 40, 60, and 80% of the maximum temperature from the same dataset. (For interpretation of the references to color in this figure legend, the reader is referred to the web version of the article.)

requires a mapping of the temperature from the non-uniform spherical coordinates to uniform or regularly spaced grids in Cartesian coordinates. Hence the computational time of volume rendering would be at least five times more, and this estimate does not include the cost of data storage for revealing the same structures as those in Fig. 4, than using the multi-isosurfaces approach.

The multi-isosurfaces approach is useful for revealing large-scale features, as shown in Figs. 3 and 4. But it has limitations, because it is not effective in revealing the small-scale structures inside the mantle. Fig. 5 shows this limitation. There is a downwelling region in the center of the image. Yet, no information can be ascertained about the precise depth of plume limbs. In the other downwellings, their features fade into one another; there is neither clarity nor distinction of the small-scale features.

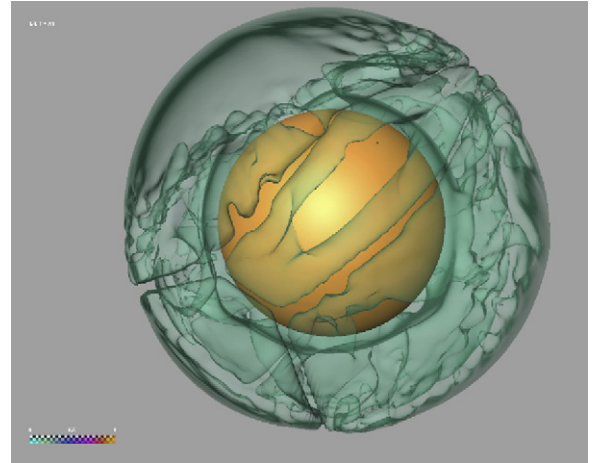


Fig. 5. Visualization of downwellings using the multi-isosurface approach for the same dataset used for Fig. 4. The isosurface has a value of 15% of the maximum temperature.

### 2.2.2. Localization of complicated small-scale features

The SelectRoi module in Amira allows the user to add two cutting planes to a 3-D object, trim off the parts that are not of interest so that a selected region of interest can be displayed. By adding the SelectRoi module to the multi-isosurfaces approach, we have been able to generate a wedge of the 3-D image instead of the entire sphere. Fig. 6 shows a quarter of the mantle, in which the downwellings are the dominant flows and last over a long time period in the simulation. The core is shown in the lower part of the Figure simply for referencing the locations of the downwelling. The data used in Fig. 6 come from the same dataset used in Fig. 4.

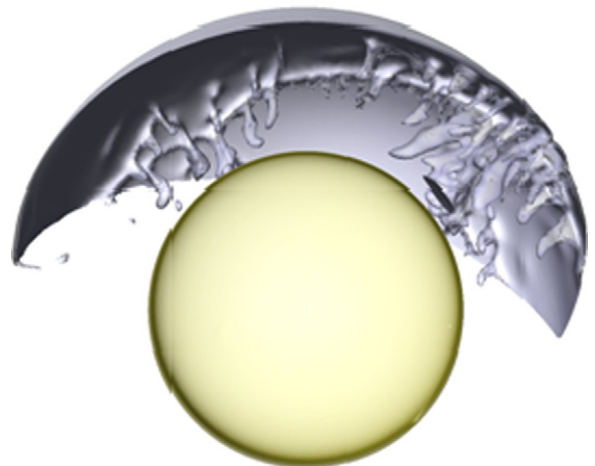


Fig. 6. View of small-scale downwellings along a long linear trench. This wedge is 1/4 of the mantle. The core is shown for marking the relative depths of the downwellings.

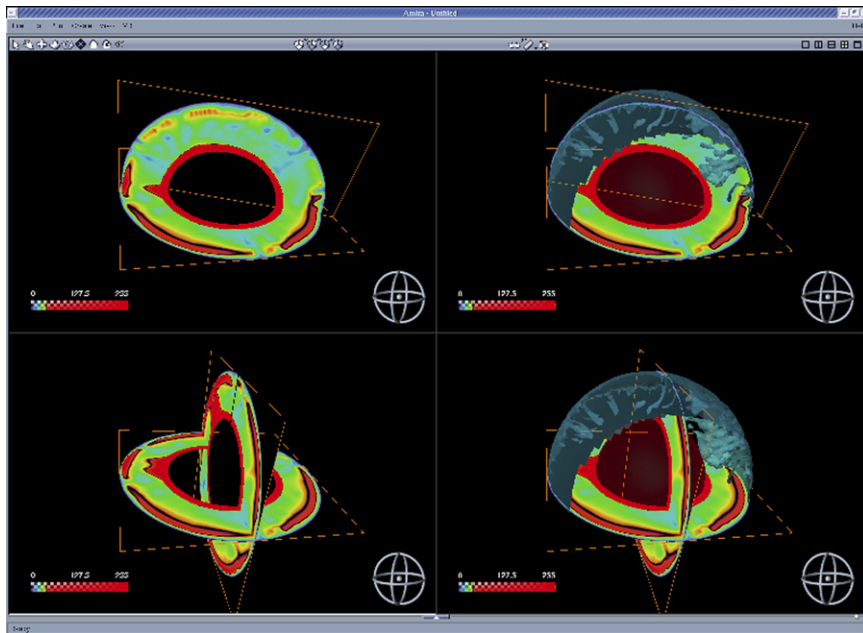


Fig. 7. Using 4-viewer mode to display different portions of the dataset by using different displaying formats.

Using the localizing approach, we have observed a new phenomenon that was not reported in previous publications according to our knowledge. The downwellings are of more complicated structures than the upwellings in the convection model with  $Ra = 2 \times 10^6$  and radially dependent viscosity (Fig. 1a) and thermal expansion coefficient (Fig. 1b). The upwellings start with several plumes growing. As the convection process develops, some of the plumes become weakened and disappear and only a few large-scale plumes survive (Fig. 4). But the downwellings consist of both large-scale features appearing as a long linear trench near the surface and small-scale sinking columns along side the long trench. While the linear trench position remains relatively stable on the surface over a long period of simulation time corresponding to the upwellings, the positions of small-scale sinking flows swing constantly on the surface, but remain close to the trench.

### 2.2.3. Use of Amira's 4-viewer mode

From the above presentation, one can sense the great challenge in visualizing the downwelling process in 3-D spherical mantle convection. That is to say that it is very difficult to show the detailed features comprehensively, using a single view. More views or more slicing or segmenting from different angles are needed to reach this elusive goal.

Amira 4.1 provides a new feature—the 4-viewer display mode, with which one can see simultaneously

different portions of the data in different displaying formats from different angles of view (Fig. 7). Each of these viewers can be independent of the others, but they can all be controlled from the same module window. We now have the ability to combine the use of multi-isosurfaces with the wedge of a region and 2-D slices in one panel to see both the movement of the sinking stalactites and the flow motions along the 2-D sections. In another panel or window we can display the downwellings, which occur on the other side of the sphere or we can have a top-down view of the same flows in the third window, etc. In short, the 4-viewer mode provides great flexibility to explore the interior complexity of the downwellings very efficiently. This 4-viewer mode is also very easy to use.

### 3. Discussion and conclusions

So far we have described the three approaches exploited from the powerful Amira graphic package for visualizing the downwelling features with different level of complexities. The multi-isosurfaces approach is good for large-scale downwellings. The wedging approach allows us to observe the details of small-scale features locally. The 4-viewer mode is the most flexible and cost-efficient tool for systematically visualizing and understanding the dynamical structures of downwellings in 3-D spherical mantle convection.

With these approaches we have observed the following interesting features that have not been reported in

previous works: (1) a long lasting convergence zone consists of many short-life small-scale downwellings, like stalactites, when viewed from the viewpoint of the core-mantle boundary; (2) persistent divergence zone is filling with cold materials in between two shrinking plumes, whose centers remain at the same locations; (3) cold material flushes into lower mantle repeatedly from the same downwelling region in the model without the presence of the endothermic phase transition.

The goal of this research work is to find an efficient way to deal with the tough problem of visualizing the downwellings in 3-D spherical mantle convection with high numerical resolution. Although the approaches presented in this paper can be very helpful, there are still technical issues challenging Amira developers. For example, one can connect the *4-viewer* mode with the movie-maker module to create a movie directly from the dataset. But this feature does not generate a movie for each of the four panels simultaneously. The movie module will generate only one movie for one of the panels. In order to create a movie for each of the panels, the images for the other three panels at each time step must be recorded by the user and then need to be recombined into different movies. This creates a substantial overhead in storage space and more is more time consuming.

Another problem that occurs with the *4-viewer* mode is the loss of resolution. Most monitors have a maximum resolution of 1600 by 1200. Dividing this resolution into four panels results in each viewer having a maximum resolution of 800 by 600. This is not very big; it is likely the small subtle features will be overlooked. To counteract this, Amira allows users to perform off-screen display of the viewers, which will increase the maximum potential resolution. The problem with this approach is that each viewer must be carried out separately and then recombined in order to create a high-resolution movie. Unless it is then displayed on a large-scale display wall, such as the Power Wall, it will lose resolution once again when it is viewed.

We have presented here some solutions to this problem of visualizing downwellings, in 3-D spherical convection, which are different from Cartesian geometry. We hope that this will help to stimulate others into looking at these interesting issues.

## Acknowledgments

We thank Larry Hanyk and Marc Monnereau for our discussions. We also thank Max Rudolph and Ben Kadlec for their reviews. Support of this research has come from NSF ITR and Middleware grants.

## References

- Baumgardner, J.R., 1985. Three-dimensional treatment of convective flow in the Earth's mantle. *J. Stat. Phys.* 39, 501–511.
- Bercovici, D., Schubert, G., Glatzmaier, G.A., 1989. Three-dimensional spherical models of convection in the earth's mantle. *Science* 244, 950–955.
- Cohen, R.E. (Ed.), 2005. High-Performance Computing Requirements for the Computational Solid Earth Sciences, 94 pp., [http://www.geo-prose.com/computational\\_SES.html](http://www.geo-prose.com/computational_SES.html).
- Cruz-Neira, C., Sandin, D.J., DeFanti, T.A., 1993. Surrounded-screen projection-based virtual reality: the design and implementation of the CAVE. *ACM SIGGRAPH* 93, 135–142.
- Davies, J.H., 2005. Steady plumes produced by downwellings in Earth-like vigor spherical whole mantle convection models. *Geochem. Geophys. Geosyst.* 6, Q12001, doi:10.1029/2005GC001042.
- Erlebacher, G., Yuen, D.A., Dubuffet, F., 2001. Current trends and demands in visualization in the geosciences. *Electron. Geosci.* 4, <http://www.msi.umn.edu/~lilli/electrongeo.pdf>.
- Fornberg, B., 1996. *A Practical Guide to Pseudospectral Methods*. Cambridge Univ. Press.
- Glatzmaier, G.A., 1988. Numerical simulations of mantle convection: time dependent, three-dimensional, compressible, spherical shell. *Geophys. Astrophys. Fluid Dyn.* 43, 223–264.
- Hanyk, L., Yuen, D.A., Matyska, C., Velimsky, J. visualization of time-dependent dynamics of postglacial rebound. *Vis. Geosci.*, in press.
- Machetel, Ph., Rabinowicz, M., Bernadet, P., 1986. Three-dimensional convection in spherical shells. *Geophys. Astrophys. Fluid Dyn.* 37, 57–84.
- Tackley, P.J., Schubert, G., Glatzmaier, G.A., Schenk, P., Ratcliff, J.T., Matas, J.-P., 2001. Three-dimensional simulations of mantle convection in Io. *Icarus* 149, 79–93.
- Zhang, S., Christensen, U.R., 1993. Some effects of lateral viscosity variations on geoid and surface velocities induced by density anomalies in the mantle. *Geophys. J. Int.* 114, 531–547.
- Zhang, S., Yuen, D.A., 1995. The influences of lower-mantle viscosity stratification on 3-D spherical-shell mantle convection. *Earth Planet. Sci. Lett.* 132, 157–166.
- Zhong, S., Zuber, M.T., Moresi, L., Gurnis, M., 2000. Role of temperature-dependent viscosity and surface plates in spherical shell models of mantle convection. *J. Geophys. Res.* 105 (B5), 11,063–11,082.